Effects of bonding on the energy distribution of electrons scattered elastically at high momentum transfer

M. Vos and M. R. Went

Atomic and Molecular Physics Laboratories6, Research School of Physical Sciences and Engineering,
The Australian National University, Canberra ACT 0200, Australia
(Received 28 June 2006; revised manuscript received 12 September 2006; published 6 November 2006)

High-resolution measurements of 40-keV electrons scattered over 44.3° from evaporated carbon films are presented. The observed width of the energy distribution of electrons scattered from carbon is significantly larger than the experimental energy resolution, and its position is shifted to lower energy. Measurements were done for transmission and reflection geometries for thin films with thicknesses varying from 90 Å to 1400 Å. The observed peak shape is largely independent of the thickness and measurement geometry. The peak shape deviates from Gaussian in all cases, in a way consistent with theories that describe these processes beyond the impulse approximation. The energy shift of the carbon peak is measured by evaporating a small amount of Au on these films. Separation of the Au and C peak is somewhat smaller than calculated assuming scattering from free C and Au atoms, but independent of measurement geometry. Finally spectra were measured from highly oriented pyrolytic graphite (HOPG) films. Now different widths are observed in reflection geometry and transmission geometry. This is attributed to the anisotropy of the motion of the C atoms in HOPG. Also the Au-C separation is slightly orientation dependent for HOPG. All observations agree at least semiquantitatively with neutron Compton scattering results, a related scattering experiment that studies neutron-atom collisions at similar momentum transfers.

I. INTRODUCTION

In this paper we want to explore the physics of keV electron scattering elastically over large angles from atoms that are part of a solid. Often the elastic peak is considered to have no intrinsic width, and hence the peak shape is considered an experimental artifact, rather than a property of the material studied. However, scattering of energetic electrons over large angles from a stationary atom implies momentum transfer from the electron to that atom. As a consequence the atom will start moving and acquire kinetic energy and the energy of the electron will be reduced by this amount. The reduction in energy will depend on the mass of the atom. If the atom is not stationary before the collision the energy lost by the electron will depend on the initial momentum of the atom ("Doppler broadening"). If we can resolve this broadening, then electron scattering can access vibrational properties in momentum space.

It will become clear that there are limitations to the validity of the very simple picture sketched above: a single atom absorbing the momentum of the scattered electrons as if it is a free atom. Indeed, asymmetries in the peaks reveal that this process is influenced by the environment of the atom. Here we want to explore our understanding of experimental observations of these very basic processes. Carbon films are the main target material, as these effects are most easily resolved for strongly bonded low-Z materials. The interpretation will be guided by extensive knowledge of neutron scattering at similar momentum transfer. These neutron experiments are often referred to as deep inelastic neutron scattering. We will, however, refer to this type of collisions as "elastic" or "quasielastic": the total kinetic energy is conserved. In this paper inelastic scattering refers to electronic excitations induced by the fast electrons.

The first high-resolution measurement of keV electrons scattered over large angles from solids was reported by Boersch *et al.* as early as 1967.[1] The object of that study was to determine if there was energy transfer from the electron to the target in large momentum-transfer collisions. He concluded that for a momentum transfer q the energy transfer was $q^2/2M$ with M the mass of the atom. In other words, the electron scatters in the case of high momentum transfer from a single atom, rather than the whole of the target. Thus it appeared, at least in first approximation, that one can describe the electron-atom collision without referring to the fact that the atom is bound in a solid. Boersch *et al.* also observed a remarkably large width of the carbon peak, which he attributed to Doppler broadening as a consequence of the motion of the carbon atoms. He assumed, in a classical way, $(3/2)kT$ kinetic energy per atom and obtained for the sample a surprisingly high temperature of 1600 K. This high temperature was attributed to beam heating, as his experiment employed quite intense beams.

At about the same time of the electron scattering experiment of Boersch *et al.* it was realized that scattering of neutrons with several eV's of energy over large angles contains signatures of the motion of atoms in liquids and solids.[2] This technique was first employed for the study of liquid helium and later, when more energetic neutron beams became available, for the study of atomic momentum distributions in solids. In this work the atomic momentum distribution was calculated using quantum physics. Even at 0 K there should be significant Doppler broadening due to the zero-point motion of atoms in a lattice.

Theories were developed (see, e.g., the paper by Sears[3]) establishing that at high momentum transfer the collision resembles that of a neutron and a free atom (i.e., the impulse approximation is valid: all particles involved in the collision

can be treated as plane waves, at least for the small time over which the collision occurs), and the observed energy distribution of the scattered neutrons can be accurately described as a Compton profile of the nuclear motion. Further, these theories predict that at lower momentum transfers the impulse approximation is not valid and corrections are required to describe the experiment. This technique, neutron Compton scattering (NCS), was reviewed by Watson[4] and, more recently, by Andreani *et al.*[5]

Often carbon, especially highly oriented pyrolytic graphite (HOPG), is used as a target to test the capabilities of the neutron experiments.[6–9] HOPG is a layered compound with very different bonding between the atoms in the hexagonal planes (strong, covalent bonds) compared to the bonding to atoms in different sheets (weak, van der Waals bonding), resulting in a large anisotropy of the vibrational amplitude. The degree to which this anisotropy is resolved is often used as a benchmark to establish the capabilities of NCS.

In more recent days the energy resolution of electron scattering experiments at keV energies has improved to the extent that the signal of light elements can be separated from that of heavy elements. This was first demonstrated for polymer films, both in transmission[10] and in reflection geometries,[11,12] where the proton signal was well clear from that of the carbon nuclei. The electron beams in this new generation of experiments are much less intense ($\simeq 1$ nA) than those employed originally by Boersch *et al.*, excluding the possibility of significant beam heating. However, the width of the carbon peak remains large,[10,13] raising doubt about the interpretation of Boersch *et al.* Indeed the width in these electron experiment appears consistent with that obtained from NCS experiment.[10]

By increasing the energy of the incoming electron beam to 40 keV and improving the energy resolution by reducing the pass energy of the analyzers, we reached the point that we can also study elastic scattering from carbon in detail. This is the subject of this paper. The experimental capabilities are demonstrated by the separation of the contribution of carbon from that of gold for an Au layer evaporated on carbon. The Au peak is much narrower than the C peak. This demonstrates that the Doppler broadening is well resolved for C. The Au-C separation is slightly smaller than expected for scattering of electrons from free atoms. This suggest that these experiments cannot be fully described within the impulse approximation. This is corroborated by asymmetries in the C peak shape. Using transmission experiments with C films over a large range of thicknesses we will show that multiple scattering has only a small effect on the measurements. Further, we will demonstrate that we can observe the anisotropy of the vibrational amplitude of C atoms in HOPG. This proves that these spectra cannot be described by classical thermal distributions, as was done by Boersch *et al.*[1] and in more recent work (e.g., see Varga *et al.*[12]). By evaporating Au on HOPG and investigating this sample for different geometries we find for HOPG a slight dependence of the Au-C peak separation on geometry. These effects cannot be attributed to multiple scattering, but are, at least semiquantitatively, in agreement with neutron scattering data and a consequence of the interaction of the carbon atoms with its environment.

II. THEORY

The foundation of the scattering theory of neutrons was firmly established in the work of van Hove.[14] For weak interacting neutrons the first Born approximation is sufficient to describe the experiment and the differential cross section is given by

$$\frac{d^2\sigma}{d\Omega d\epsilon} = AS(\boldsymbol{q}, \omega); \tag{1}$$

here, $\boldsymbol{q}$ is the transferred momentum, ω the transferred energy, and $S(\boldsymbol{q}, \omega)$ the dynamical structure factor, a property of the target. The dynamical structure factor used here refers to energy loss and momentum transfer to the nuclei and is different quantity from the dynamical structure factor of the electron gas, a quantity often studied in electron energy loss spectroscopy. The quantity A is determined by the geometry and is given by (using atomic units)

$$A = \frac{m^2}{4\pi^2} \frac{k_1}{k_0} V(\boldsymbol{q})^2; \tag{2}$$

here, m is the mass of the scattered particle, $\boldsymbol{k}_0$ and $\boldsymbol{k}_1 = \boldsymbol{k}_0 - \boldsymbol{q}$ the initial and final momenta of the scattered particle, and $V(\boldsymbol{q})$ the Fourier transform of the particle-target interaction.

If the electron experiment can be described by the first Born approximation, then the only difference is in the factor A. It depends on the atom one scatters from, but it is further a constant of the experiment (for electrons the phase-space factor $k_1/k_0 \simeq 1$ is an excellent approximation, and for neutron experiments $k_1/k_0 = \sqrt{E_1/E_0}$ deviates from 1 but can be incorporated fully in the analysis; see, e.g., Ref. [15]). Thus if one scatters from a target that consists of a single element, then one expects for experiments arranged in such a way that the same momentum transfer $\boldsymbol{q}$ occurs, the same shape of the spectra in an electron and neutron experiment. This implies that spectra obtained from scattering experiments of keV electrons should contain the same information as spectra obtained from scattering experiments of neutrons with several eV energy. Conversely, deviations in the observed shape in both experiments could be interpreted as a failure of the first Born approximation to describe the electron experiment. This is quite well possible, as, for example, elastic cross section calculations based on the first Born approximation are, even at these energies, only considered a rough approximation. For a more detailed comparison of the electron and neutron experiments, as applied to polymer films, see Ref. [16].

In the context of neutron experiments it was established that the time τ over which the scattered particle interacts with the target is given approximately by

$$q v_0 \tau = 1, \tag{3}$$

with v_0 the root-mean-square velocity of the scattering atom.[3] For sufficiently large q the displacement of the scattering atom, during this time τ, is so small that it effectively does not probe the lattice potential during the collision. Under these conditions the collision appears to be between two free particles: i.e., the impulse approximation is valid. Then $S(\boldsymbol{q}, \omega)$ simplifies to $J(y)$, a function of only one variable

with $y = \frac{M}{q}\left[\omega - \frac{q^2}{2M}\right]$, and the measured distribution, centered at $y = 0$, is simply a Compton profile of the nuclear motion. y can then be identified as the component of the target atom momentum along the direction of transferred momentum $\hat{q}$: $y = \hat{q} \cdot \mathbf{p}$ with $\mathbf{p}$ the momentum of the atom the probing particle is scattered from before the collision. $J(y)$ is then the probability that the scatterer has a momentum component y along the direction of momentum transfer. In this limit the energy loss of a particle scattered from an atom with mass M and momentum $\mathbf{P}$ is simply the classical recoil energy E_r:

$$E_r = \frac{q^2}{2M} + \frac{\mathbf{q} \cdot \mathbf{p}}{M}. \tag{4}$$

The kinetic energy of the atom before the collision is $(p_x^2 + p_y^2 + p_z^2)/2M$. For a polycrystalline sample all three directions are equivalent and the total kinetic energy can be obtained from just one measurement;

$$E = \frac{3}{2M} \int_{-\infty}^{\infty} y^2 J(y) dy, \tag{5}$$

and is thus proportional to the square of the second moment of the measured distribution. For a single crystal one has to make measurements with $\mathbf{q}$ aligned with three perpendicular directions to obtain the mean kinetic energy. In the case of HOPG (ordering of the c axis only) we have only two directions, which are not equivalent. If we position HOPG with $\hat{q}$ perpendicular to the hexagonal planes, then the Doppler shift is determined by the momentum component perpendicular to the planes, and we can determine $p_\perp^2/2M$: from the second moment of $j_\perp(y)$,

$$\left\langle \frac{p_\perp^2}{2M} \right\rangle = \frac{1}{2M} \int_{-\infty}^{\infty} y^2 J_\perp(y) dy, \tag{6}$$

and a similar expressions is obtained for the crystal orientations with $\hat{q}$ parallel to the hexagonal planes:

$$\left\langle \frac{p_\parallel^2}{2M} \right\rangle = \frac{1}{2M} \int_{-\infty}^{\infty} y^2 J_\parallel(y) dy. \tag{7}$$

The total kinetic energy E of a carbon atom is then $E = 2\langle p_\parallel^2/2M \rangle + \langle p_\perp^2/2M \rangle$.

At intermediate momentum transfers the spectra can be described by a Compton profile plus correction terms.[3] These terms are referred to as final-state effects, as they are caused by the fact that the probing particle-nucleus collision cannot be accurately described as a collision between free particles. Incorporating the first nonzero correction term to the impulse approximation Sears obtained[3]

$$S(\mathbf{q}, \omega) = \frac{M}{q}\left[1 - \frac{m\Delta V}{36q} \frac{d^3}{dy^3}\right] J(y), \tag{8}$$

where ΔV refers to the Laplacian with respect to the position of the scattering atoms of the total potential energy of the system. In practice one chooses $J(y)$ usually to have a Gaussian shape. Asymmetric peak shapes are a sign that corrections to the impulse approximation are resolved. We want to investigate if this correction term, which is well established in neutron scattering, can be resolved for electron scattering.

III. EXPERIMENTAL DETAILS

Thin evaporated carbon films were supplied by Arizona Carbon Foil Company with a nominal thickness between 2 and 32 μg/cm^2 (using the density of graphite this corresponds to thicknesses between 90 Å and 1400 Å). The films were floated off from their glass support in distilled water and subsequently transferred on a shim with 2-mm holes. These samples were introduced into the electron momentum spectrometer, extensively described in Ref. [17]. The spectrometer was used in this work for elastic scattering. The carbon films were annealed by electron bombardment up to about 600–900 °C, to ensure it was conductive and to clean it from adsorbates. This also increases the long-range order in the film, as judged from diffraction. Hence, for the purpose of this paper one can think of these films as polycrystalline, rather than amorphous, but the annealing temperature is not enough to fully establish long-range order. Sometimes a 0.5–2-Å-thick Au layer was evaporated on this film (thickness judged from a crystal thickness monitor reading); the pressure during evaporation was in the 10^{-6} Pa range. After evaporation the sample was transferred under vacuum to the main chamber (pressure in the 10^{-9} Pa range).

Here the electron gun emits a beam of 500 eV energy and the sample is in a semisphere kept at +39.5 keV. Thus a 40-keV electron beam of 0.2–1 nA impinged on the sample. The momentum $|k|$ of a 40-keV electron is 104.4 Å^{-1}, or 54.6 a.u. (1 a.u. of momentum corresponds to 0.529 Å^{-1}). The detector is placed at $\theta = 44.3°$. Hence the magnitude of the transferred momentum is given by $\mathbf{q} = 2k_0 \sin \theta/2 = 41.2$ a.u. (77.9 Å^{-1}) [see Fig. 1(b)]. The measurements were done either in a reflection geometry or a transmission geometry. In both cases part of the beam was transmitted through the sample and collected in a Faraday cup behind the sample [see Fig. 1(a)]. The beam diameter (0.1 mm) is much smaller than the 2-mm holes. Even when we use a support shim with 0.3-mm holes we do not detect counts in the analyzers if there is no film covering the holes. Hence we are confident that in this case, using 2-mm holes, no electrons scattered from the support shim are detected, even when we come in or out at a relatively glancing angle of $\simeq$22.2°. The scattered beam is decelerated and focused by electrostatic lenses and enters the hemispherical analyzer, kept at −300 V and operating at a pass energy of 200 eV.

In order to get good energy resolution we used as a filament a barium oxide dispenser (supplied by Heatwave Labs Inc., model 311M), operating at a very low heating current (0.67 A). A typical spectrum is collected in about 1 h.

The performance of the spectrometer is tested using a self-supporting Au film. As Au is a heavy atom, we expect broadening of the elastic peak due to its thermal motion to be negligible [see Eq. (4)]. Due to its high Z (and hence large elastic scattering cross section), spectra could be taken with an extremely low beam current (0.05 nA, rather than the 0.5–1.0 nA used for the measurements on C films). The Au measurements were done using a dispenser heating current of
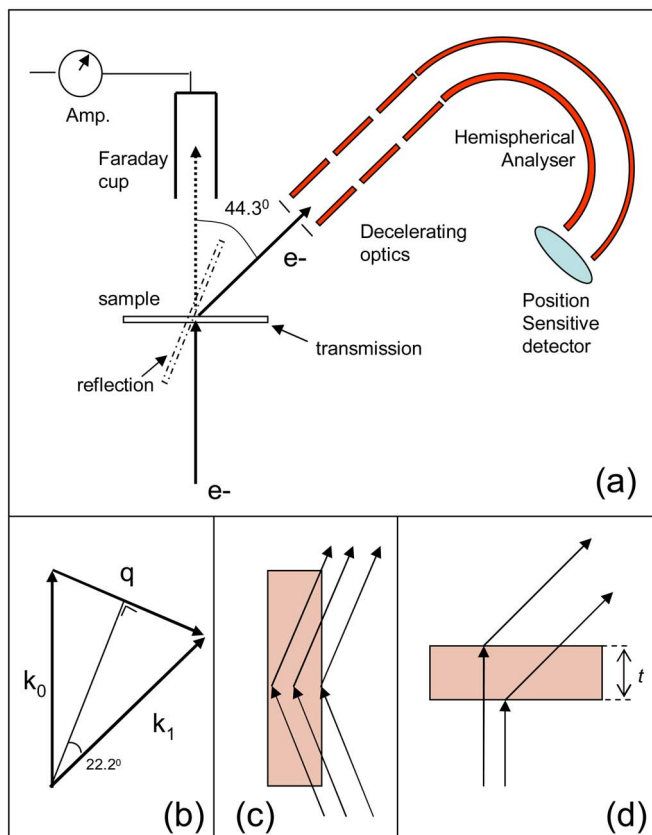
FIG. 1. (Color online) Schematic of the measurement geometry: (a) 40-keV electrons scatter over $\theta_s = 44.3°$ from a thin sample (either in transmission or in reflection) and are decelerated to the pass energy of 200 eV and analyzed for energy by the hemispherical analyzers. In (b) we illustrate that the transferred momentum $q = 2k_0 \sin \theta/2$. In (c) and (d) we show that in a reflection geometry a wide range of trajectory lengths contribute [from zero length to $2t/\sin(\theta_s/2)$], whereas in the transmission geometry the minimum length is t and the maximum length is $t/\sin\theta_s$.

0.563 A, 0.660 A, and 0.699 A. The results are shown in Fig. 2. All peak shapes are asymmetric, the measurements taken with high-filament current more so than those taken at lower filament current, and a Gaussian fit clearly does *not* describe the data well. The temperature dependence suggests that the Maxwell-Boltzmann energy distribution of the emitted electrons is reflected in the shape of the elastic peak. We fitted the peak with the convolution of a Gaussian and a Maxwell-Boltzmann energy distribution, with temperature (presumably of the filament) as fitting parameter. The Gaussian contribution was fairly independent of filament current (0.27 eV FWHM ±5%); the temperature obtained from the fit increased from 771 K at 0.56 A to 994 K at 0.7 A. These temperatures appear consistent with values quoted by the manufacturer at much larger heating currents (1170 K at 0.9 A, 1270 K C at 1 A). All other measurements reported here were done at a filament current 0.67 A for which a temperature of 914 K was obtained from the fit.

The interpretation mentioned in the Introduction assumes no multiple scattering. For electrons, interacting strongly with a target, this is most likely an oversimplification. We 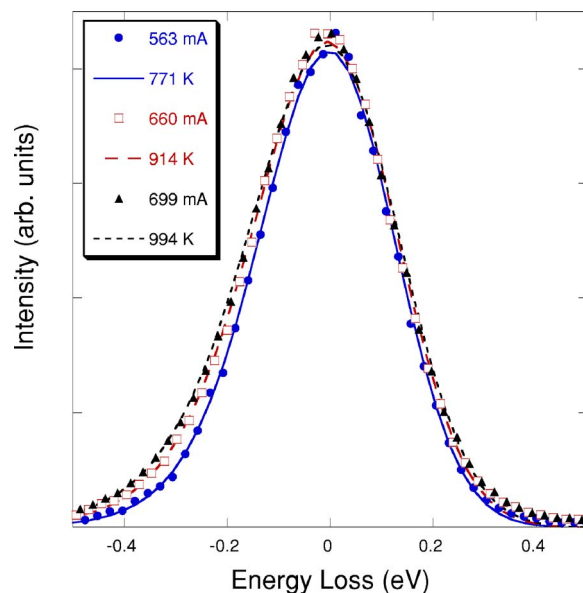explore experimentally the effects of multiple scattering using transmission experiments with varying foil thicknesses t. In a reflection experiments one has contributions from trajectories with length l varying from zero (scattering right at the surface) to $l = 2t/\sin(\theta/2)$ [Fig. 1(c)]. However, elastically scattered electrons only contribute to the elastic peak if no inelastic scattering occurs. This probability decreases with l as $e^{-l/\lambda}$ with λ the inelastic mean free path (IMFP). For 40-keV electrons in carbon the IMFP is about 400 Å. Hence for thicker films most of the signal in the reflection geometry originates from depth $t < \lambda \sin(\theta/2)/2 \simeq 80$ Å and the spectra are not expected to change anymore if the thickness is increased beyond $t \simeq 200$ Å. For a transmission experiment the trajectory length, in a single scattering approximation, varies from $l = t$ (scattering at the exit surface) to $l = t/\cos \theta$ [Fig. 1(d)]. Increasing the film thickness to values much larger than the IMFP will cause a decrease in count rate in the elastic peak region, putting an upper limit to the thickness of the film one can study (in practice around 5 times the inelastic mean free path). The average trajectory length t of events contributing to the elastic peak in transmission mode is less than in reflection geometry if $t < \lambda$ but larger if $t > \lambda$. Hence this larger variation in length makes transmission experiments using targets with a range of thicknesses very well suited for the study of the importance of multiple scattering.

FIG. 2. (Color online) Au elastic peak, taken at different filament currents [0.563 A (•), 0.660 A (□), 0.699 A: (▲)], and their fit of a convolution of a Maxwell-Boltzmann energy distribution and a Gaussian. The Gaussian had a full width half maximum (FWHM) of 0.27% ±5% eV and the temperature of the Maxwell-Boltzmann distribution is indicated.
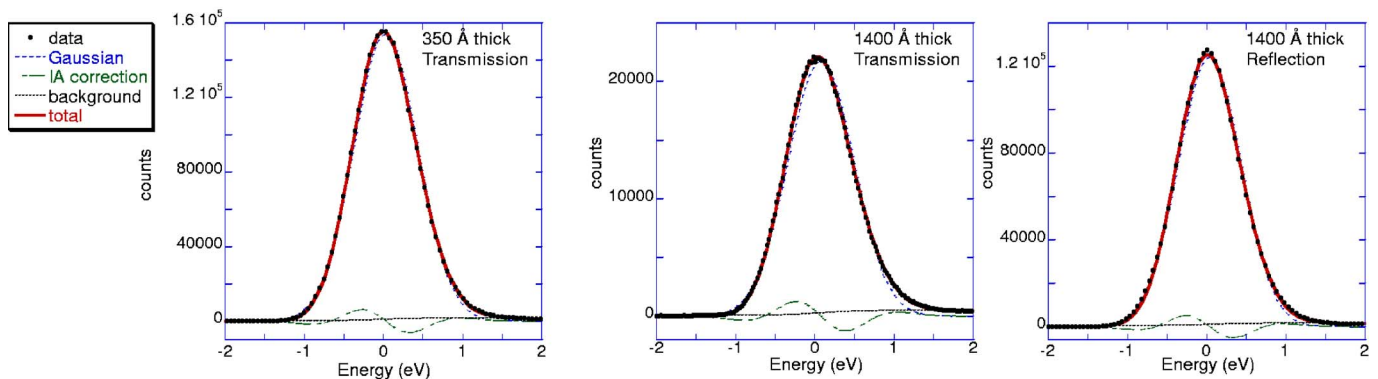
IV. EXPERIMENTAL RESULTS

A. Shape of the elastic peak in polycrystalline carbon

The zero point of the energy scale of our spectrometer is somewhat dependent on the sample position, as small changes in sample position change the path of the elastically scattered electrons through the detector which shifts the en-
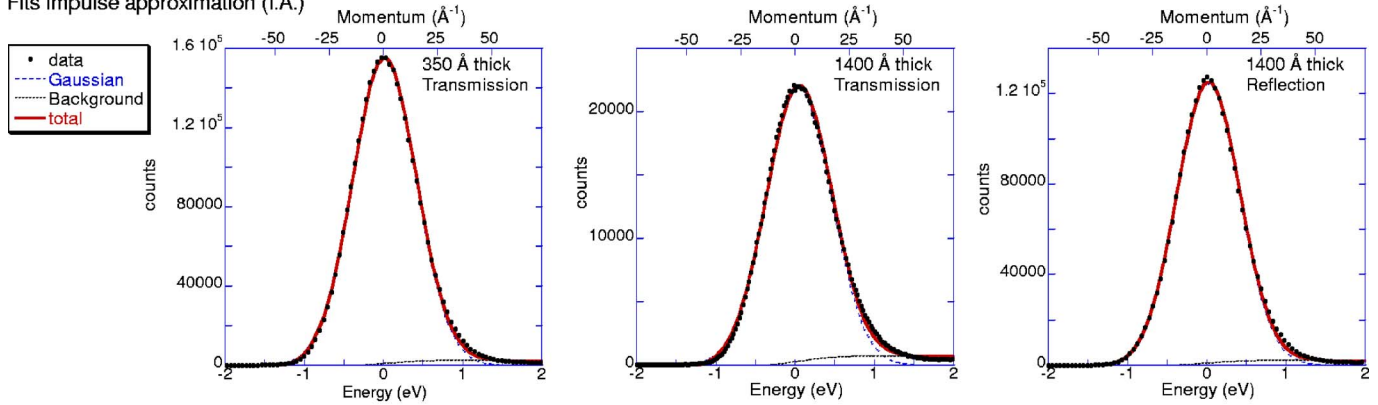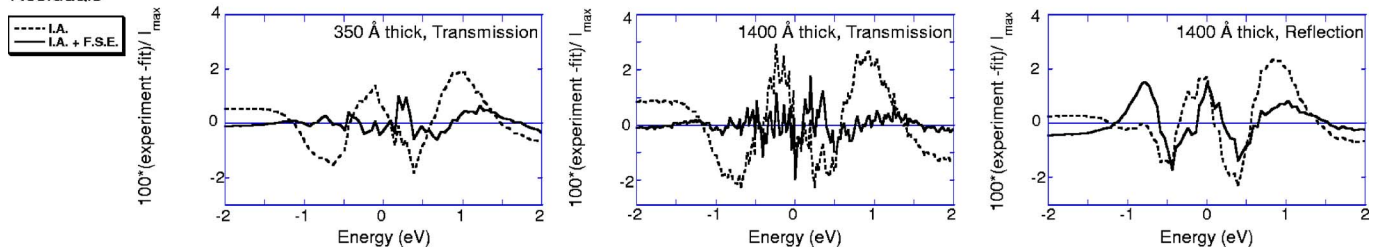
FIG. 3. (Color online) The fits of the spectra obtained in transmission for a 350-Å-thick and a 1400-Å-thick carbon sample, as well as those obtained in a reflection geometry for a 1400-Å-thick sample. In the top row the fit consists of a Gaussian plus a background (impulse approximation); the central row is a fit including final-state effects. The bottom row shows the residuals for both fits.

ergy scale; hence, it is not possible to compare the energy positions of measurements that had the sample realigned (with 0.2 mm accuracy). The electron emitter work function also depends slightly on the heating current and cleanliness of the filament which in turn affects the absolute energy scale, and there are small long-term variations in the residual magnetic field present in the spectrometer. For these reasons we split our study of the elastic peak into two parts. In the first part the sample is pure carbon, and we focus on width and peak asymmetry. On the second part we use an evaporated Au marker to establish the approximate zero point of the energy scale.

Some results for carbon films are shown in Fig. 3. The peaks are plotted in such a way that maximum intensity correspond to 0 eV energy loss. Thus at 0 eV one scatters from a target atom with no momentum along q. Clearly the carbon peaks are much broader than those of Au (Fig. 2), and hence

the Doppler broadening is indeed well resolved in these experiments. The momentum component of the atom along q can thus be obtained from the data by scaling the energy loss value by q/m [see Eq. (4), top horizontal axis in Fig. 3].

As a most basic approach one would fit the data with a Gaussian $c_I G(\epsilon, c_s, c_w)$. Here the c_s is a fitting constant determining the position of the Gaussian; this fitting parameter is required due to the uncertainty in the zero of the energy scale of our spectrum, and c_w represents the width of the Gaussian and c_I its intensity. However, especially for thicker films, the intensity does not approach zero for large energy loss values. This is due to electronic excitations (inelastic scattering). Part of the electrons scattered over 44.3° have lost a small amount of energy due to electronic excitation occurring before or after the deflection. There are peaks in these energy loss distributions near 6 and 25 eV, due to the so-called π and σ plasmons. There appears to be no clear

TABLE I. The obtained values for σ and ΔV for carbon films of thicknesses and geometry as indicated, as well as for the HOPG measurement discussed in Sec. IV D. Also the observed separation of the Au and C elastic peak, $\Delta \epsilon$, is given. Straight application of Eq. (4) yields $\Delta \epsilon = 1.03$ eV.

		Geometry				
		Transmission			Reflection	
t						
(Å)	σ (eV)	ΔV (eV Å^{-2})	$\Delta \epsilon$ (eV)	σ (eV)	ΔV (eV)	$\Delta \epsilon$ (eV)
90	0.43		0.90	0.41		0.88
350	0.41	96	0.94	0.40	81	0.92
700	0.41		0.92	0.41		0.92
1400	0.42	149	0.88	0.40	48	0.91
HOPG	0.46		0.91	0.35		0.97

structure in the energy loss distribution over the first few eV energy loss. Hence the background is approximated by a Shirley background: the intensity of the background at energy ϵ is proportional (constant of proportionality c_B) to the area of the elastic peak with energy loss less than ϵ.[18] Furthermore, there is a very small, constant intensity observed for negative energy loss values. This is the dark count rate of the multichannel plates, and this introduces an additional fitting constant c_0 giving a contribution independent of energy. The first attempt to fit the data was thus

$$I_{IA}(\epsilon) = c_0 + c_I G(\epsilon, c_s, c_w) + c_B \int_{-\infty}^{\epsilon} G(\omega, c_s, c_w) d\omega. \quad (9)$$

The results of the fits are given in Table I. The width (standard deviation) obtained for the reflection geometry is constant, 0.407 ± 0.004 eV, but in transmission it increases gradually from 0.406 (350 Å) to 0.417 eV (1400 Å). The latter increase is attributed to multiple scattering. Its effect on the width is small, only about 3%. The only exception is the thinnest film measured (90 Å) which has the largest width (0.429 eV). The different behavior for extremely thin films is probably due to surface impurities (notably due to the releasing agent containing Na atoms, used to ensure that the carbon film can be floated off its glass substrate), whose contribution becomes a larger fraction of the total intensity with decreasing carbon film thickness.

However, there were very reproducible systematic errors in the fit, for all thicknesses and in both reflection and in transmission geometries. Hence, for the cases were we had good statistics (maximum >10 000 counts) we expanded the fit to include final-state effects [see Eq. (8)] by the addition of the third derivative of the Gaussian multiplied by c_F:

$$I_F(\epsilon) = I_{IA} - c_F \frac{d^3}{d\epsilon^3} G(\epsilon, c_s, c_w). \quad (10)$$

The inclusion of final-state effects (FSE's) involves only one additional fitting parameter c_F, but as is seen from the lowest panel of Fig. 3, this one parameter removes the majority of the structure of the residuals and often only noise remains. The dramatic improvement of the fit is also obvious if one plots the spectra on a 10× expanded vertical scale, as is done in Fig. 4. The position of the Gaussian peak in the fit shifts by ≈0.03 eV to larger energy loss values with FSE included,

compared to position obtained in the impulse approximation, but the obtained width is hardly affected by the inclusion of the FSE term.

B. Position of elastic peak in polycrystalline carbon

In this second part we want to determine the peak position of the carbon peak. For this purpose a Au marker was evaporated on the C film. The Au shift is very small [0.06 eV according to Eq. (4) for $\mathbf{q} = 41.2$ a.u.]. We think it is reasonable to assume that the energy shift of Au as calculated from Eq. (4) is accurate within 20% (0.01 eV). Thus deviations of the observed Au-C splitting compared to the calculated one [using Eq. (4)] are attributed to deviations in the carbon shift.

After evaporation of a small amount of Au on the carbon films we observe two clear peaks (see Fig. 5), one with approximately the same width as obtained for the free-standing Au film and one at larger energy loss with the same width as the carbon peak before Au evaporation. According to Eq. (4)
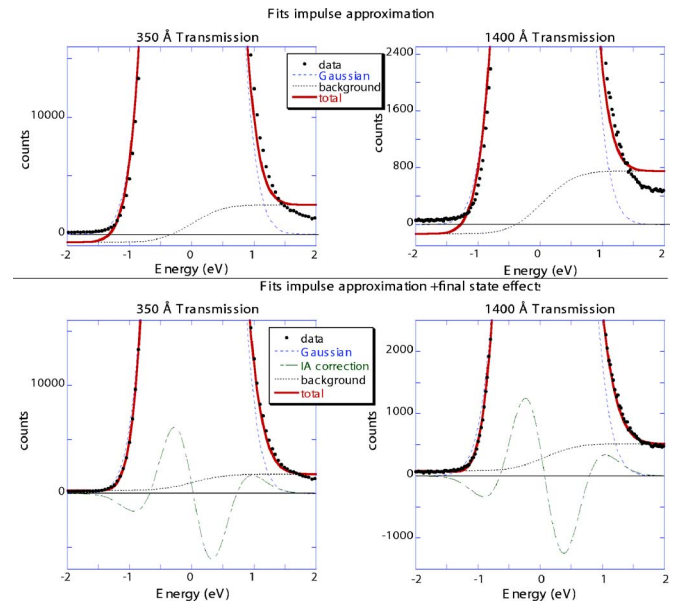

FIG. 4. (Color online) The same as Fig. 3 but now with a 10× enlarged vertical scale. Only the two transmission experiments are shown. The top two fits use a Gaussian and a background. The lower two fits include final-state effects as well.
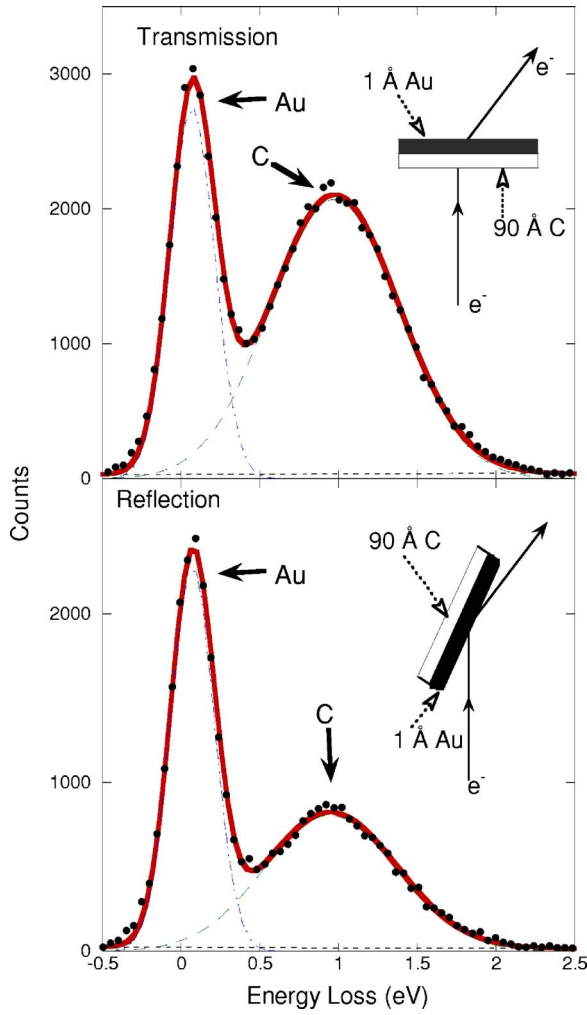
FIG. 5. (Color online) An example of the elastic peaks after evaporation of Au on amorphous C. Here we evaporated approximately 1 Å on 90-Å-thick carbon film. Measurement geometry as indicated. The fact that the Au/C peak ratio is larger for the reflection measurement than the transmission experiment is a consequence of the fact that in the reflection case the back of the carbon film does not contribute very effectively, as the signal of these atoms is, even for a 90-Å-thick film, severely attenuated by inelastic scattering.

the energy separation of the C and Au peak should correspond to 1.03 eV (shift is 1.096 and 0.066 eV for C and Au, respectively). The observed splitting $\Delta\epsilon$, obtained by just fitting the spectra with two Gaussians, is given in Table I. Except for the thinnest sample (where the contributions to the signal of surface impurities with intermediate Z appears to be significant, affecting the C peak width and causing a decrease in Au-C separation) there is a small decrease in separation with increasing thickness for the transmission geometry, whereas for the reflection geometry the separation is fairly constant. The latter is expected as effectively only the outermost layers are probed in the reflection geometry, and hence increasing the thickness does not change the signal. For the transmission geometry the decreasing separation could be due to multiple scattering. A similar decrease in separation was observed in Monte Carlo simulations of the separation of C and H in polyethylene.[12] This decrease in separation with increasing thickness is only a very minor effect. The separation value obtained for the 350-Å-thick film (0.94 eV) is slightly less than the calculated value (1.03 eV). However, these fits were based on Eq. (9), and we have seen that fitting of a carbon peak using Eq. (10) causes a shift of the Gaussian of 0.03 eV. Thus the difference between observed and calculated Au-C splitting appears to be only in part due to final-state effects.

C. Comparison with neutron scattering results

The observed peak width, shown in Table I, of carbon was first corrected for experimental resolution by subtracting in quadrature the width of the Au peak ($\sigma_{int}=\sqrt{\sigma_{obs}^2-\sigma_{Au}^2}$, $\sigma_{Au}\simeq 0.15$ eV). The resulting intrinsic carbon width σ_{int} can be translated to the mean kinetic energy of the carbon atoms for the polycrystalline film using Eq. (5). This result is given in Table II together with estimates obtained from neutron scattering. The agreement is satisfactory.

From the asymmetry we can, using Eqs. (8) and (10), obtain another property of carbon: ΔV. This is much more challenging as this quantity is determined from a small asymmetry in the peak shape. Hence the spread obtained for the different films (see Table I) and the much larger quoted error in this quantity in Table II. The value obtained from electron scattering is of the right order of magnitude, but

TABLE II. The values obtained for the mean kinetic energy and ΔV for polycrystalline graphite and HOPG as obtained by different authors. The value given for the 1967 results of Boersch *et al.* (Ref. 1) was calculated from his 90° scattering results for 30-keV electrons and 150-K sample temperature. Errors in the current work are based on variations between the results obtained from different samples.

Ref.	Probe	graphite, poly E (meV)	ΔV (eV Å^{-2})	$\langle p_\perp^2/2M \rangle$ (meV)	HOPG $\Delta V_\perp$ (eV Å^{-2})	$\langle p_\parallel^2/2M \rangle$ (meV)	$\Delta V_\parallel$ (eV Å^{-2})
1	e^{-1}	70					
6	n			24±1		45±2	
7	n			24±1		43±2	
19	n	108.3±3.0					
20	n	91.3±0.3	124.8±4	19.02±0.07	35.6±1.4	36.8±0.1	200±2
Cur.	e^{-1}	101±10	100±50	23±4	40±15	42±8	180±60

somewhat smaller than that obtained from neutron scattering. Determination of ΔV is clearly at the limit of what is possible with the present spectrometer.

D. Peak width and position in HOPG

Finally we want to investigate if we can resolve the anisotropy of the vibrational amplitudes in highly oriented pyrolytic graphite. By rotating the crystal over 90° we can change the direction of q from along the graphite sheets to perpendicular to these sheets. One of these two measurements is necessarily a transmission experiment, the other a reflection measurement. Thin HOPG samples were prepared by cleaving using sticky tape followed by in-vacuum annealing. Due to the completely different nature of sample preparation, it is not possible to specify the thickness accurately. Several different thinned samples were prepared with thicknesses varying between $\simeq 500$ Å and $\simeq 1200$ Å (as judged from the degree of transparency and intensity at the first plasmon peak in the energy loss spectrum). Clear diffraction patterns were observed (the sizes of the crystallites in HOPG were similar to the electron beam size; with some care single-crystal diffraction could be obtained with sixfold symmetry). Furthermore, an $(e,2e)$ spectrum taken with this sample showed strong suppression of the π band, another sign of alignment of the hexagonal planes.[21] For the reflection experiment we have both used a separate, thick sample or, in one case, a cleaved thinned sample could be used. The measurement geometries and some results for the HOPG experiment are shown in Fig. 6. The transferred momentum is either along the graphite planes (transmission measurement) or perpendicular to the graphite planes (reflection measurement).

The reproducibility between the different measurements was not as good as the reproducibility of the annealed amorphous carbon experiments. However, the carbon peak was in all cases clearly wider for the geometry with q along the graphite planes (varying between $\sigma = 0.44$ eV and $\sigma = 0.47$ eV), compared to perpendicular to the planes (varying between $\sigma = 0.34$ eV and $\sigma = 0.36$ eV). Typical values are given in Table I. We attribute the larger variability of these measurements to different degrees of wrinkling of the films and the presence of partly cleaved layers, still connected at one side to the main film, but with a different orientation. The latter could sometimes be observed under an optical microscope.

This change in peak width can be understood from the crystal structure. The carbon peak is tightly bonded in the plane, and in the plane the nearest neighbors are only a small distance away. The carbon atom is, in the directions of the graphitic plane, very localized in coordinate space and, consequently, delocalized in momentum space. Perpendicular to the planes the potential well is less steep, causing delocalization in coordinate space and a narrow distribution around zero in momentum space. Besides the difference in width it is clear from Fig. 6 that from the transmission measurement the peak is also more asymmetric. For this measurement the final-state effects are even more pronounced that for the annealed amorphous carbon films. Fits for this measurement
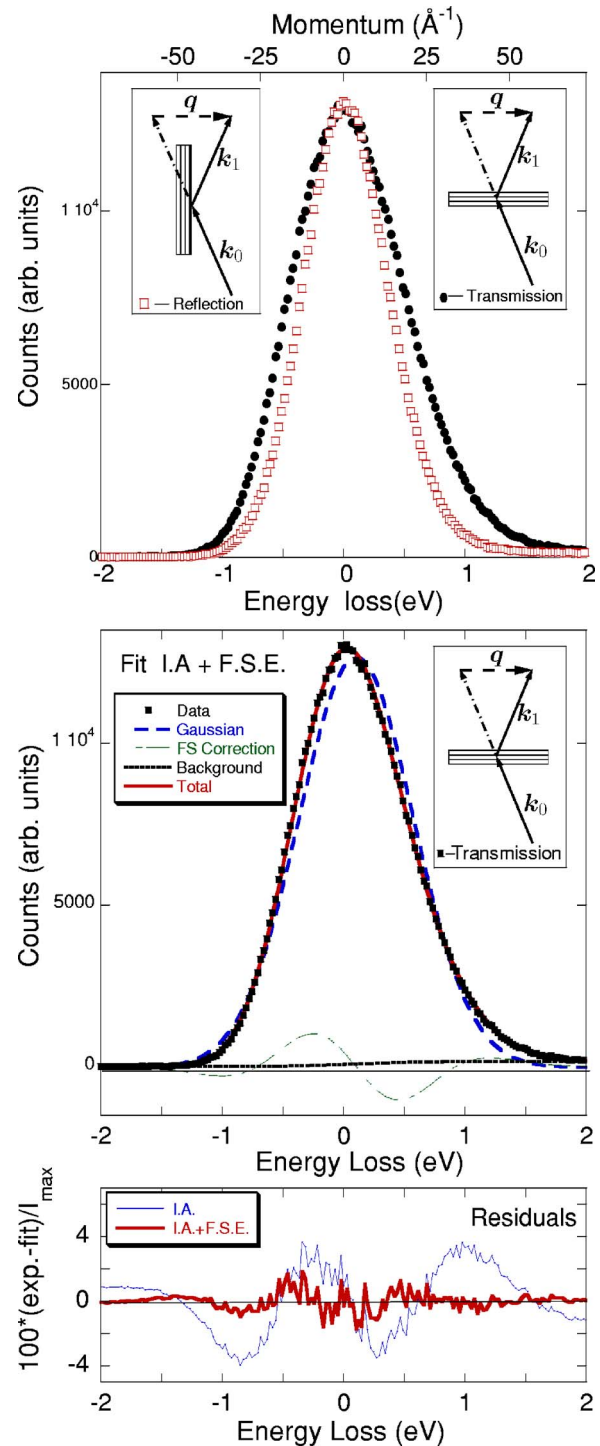

FIG. 6. (Color online) HOPG elastic peak measured with q along (•) and perpendicular (□) to the graphite sheets. The measurement with q along the graphite plane is broader and more asymmetric. For a satisfactorily fit this spectrum requires large final-state corrections (see central panel, only fit with final-state corrections shown). Residuals of this fit with and without final-state effects are shown in the bottom panel.

geometry including final-state effects are shown in the central panel of Fig. 6. The residuals of a fit with and without final-state effects are shown in the bottom panel. Clearly including the final-state effects improves the fit dramatically.

For the measurement with q perpendicular to the graphite sheets a much smaller contribution due to final-state effects was found. The results of our first attempts to derive values for ΔV are given in Table II. The obtained values for ΔV as derived from the peak asymmetry have again a considerable error. However, there is a large difference between the values obtained for ΔV for the two measurement geometries. Thus the anisotropy of this quantity is resolved as well. This strong orientation dependence of the final-state effects was also observed in neutron scattering.[20] For momentum transfer along the c axis the atom is in a broad potential minimum and scattering resembles that of scattering from a free atom. For q perpendicular to the c axis the particle probes the in-plane potential, which is much steeper, and hence larger deviations from the impulse approximation are expected.

From the two measurement geometries we obtain the values for HOPG of $\langle 2p_\perp^2/2M \rangle$ and $\langle 2p_\parallel^2/2M \rangle$ using Eqs. (6) and (7). These values are given in Table II as well. The current results are closer to the earlier neutron experiments than the most recent neutron experiment, and the agreement is such that it is obvious that the neutron and electron experiments capture, at least in first order, the same physics.

We evaporated a small amount of Au on the sample and measured the spectra again to establish the energy scale and check that the different width was not due to variations in spectrometer performance. For the reflection experiment 0.2 Å of Au caused a peak of similar intensity as the carbon peak, as we are in this geometry quite surface sensitive. For the transmission case we evaporated 2 Å of Au. The Au peak width was independent of the crystal orientation and similar to the Au peak of the free-standing film, but again the carbon peak width varied. The Au-C splitting varied from 0.90 eV to 0.93 eV for q perpendicular to the graphite planes and from 0.95 to 0.98 for q along the graphite planes. Thus not only is the width of the carbon peak dependent on the HOPG orientation, but it appears from Fig. 7 that also the Au-C separation differs for the two orientations by between 0.02 and 0.08 eV. Again the variation in results indicate that the size of these effects are on the limit of what we can determine with the current spectrometer. The change in separation can be attribute to the apparent carbon peak shift due to the anisotropy of the final-state effects. However, the calculations show that the values of the final-state effects derived from the peak asymmetry causes an apparent shift of the peak position of only $\simeq 0.03$ eV—i.e., in agreement with the lower limit of the experimentally found variations.

V. CONCLUSION AND DISCUSSION

We have demonstrated that much of the elastic scattering from electrons of carbon at high momentum transfer can be understood using the same physics as neutron scattering at similar momentum transfer. There are small effects of multiple scattering, but the mean kinetic energy for polycrystalline carbon films is in line with that obtained from neutron scattering. The energy shift was determined from the position of the Au and carbon elastic peak. The energy separation obtained ($\simeq 0.94$) was somewhat less than that expected for scattering from free carbon and gold (1.02 eV). Inclusion of
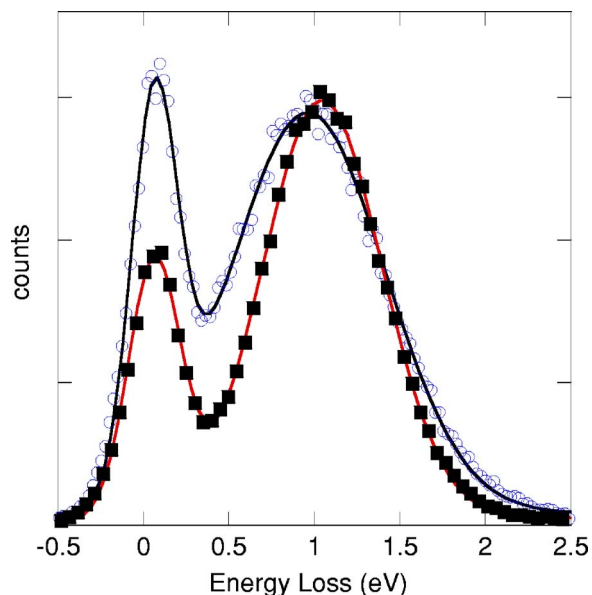

FIG. 7. (Color online) The elastic peak of HOPG with 0.2 Å Au evaporated on it, measured in a reflection geometry (■), and thin HOPG with 2 Å of Au measured in a transmission geometry (○). In the first case q was along the graphite planes, in the second case perpendicular. The solid line is the result of a fit with two Gaussians. The peak at 0.06 eV energy loss is due to electrons scattered from Au, the peak at around 1 eV energy loss due to electrons scattered from C. Note the difference in width *and* position of the carbon peak for both measurement geometries.

final-state effects improves agreement somewhat, but a discrepancy of about 0.05 eV remains. The peak shape of carbon is clearly affected by final-state effects, but the magnitude of this small effect is somewhat smaller than that obtained from neutron scattering. Further, it is demonstrated that the elastic peak width for HOPG is dependent on the angle between the graphite planes and the momentum transfer. This is a clear proof that the momentum distribution of carbon in graphite *cannot* be described by a thermal Maxwell-Boltzmann distribution. The orientational dependence of the width of the elastic peak for HOPG is much larger than the effect of multiple scattering. Finally it was found that after evaporation of a Au overlayer the Au-C peak separation also depends slightly on the HOPG orientation. This is again qualitatively in line with neutron Compton results, as final-state effects are much stronger for q along the graphite planes compared to perpendicular to the graphite planes.

There is thus little doubt that neutron scattering and electron scattering at high momentum transfer both probe $S(q, \omega)$ and thus a study of the neutron scattering literature is very helpful in the interpretation of the electron experiments. This is an important fact and opens the possibility of the use of electrons to probe $S(q, \omega)$ for targets that cannot be easily studied by neutrons (e.g., for gas-phase molecules the electrons experiment is straightforward[22]).

There is one aspect that is not discussed in this paper: the ratio of the intensity of the Au and C peaks. This question will be dealt with in a separate paper. From an applied point of view this may be an important question since this tech-

nique has obvious potential for quantitative surface analysis, especially if more elements can be separated from each other. This is an important motivation for our planned studies at higher momentum transfer.

Finally we want to mention two papers dealing with the theory of electron scattering at high momentum transfer. One was published in 1983 by Bonham and de Souza[23] and more recent work by Fujikawa *et al.*[24] These papers approach the problem from different point of views, and the overlap with theory, as described in this work, is not obvious.

[1] H. Boersch, R. Wolter, and H. Schoenebeck, Z. Phys. **199**, 124 (1967).

[2] P. C. Hohenberg and P. M. Platzman, Phys. Rev. **152**, 198 (1966).

[3] V. F. Sears, Phys. Rev. B **30**, 44 (1984).

[4] G. I. Watson, J. Phys.: Condens. Matter **8**, 5955 (1996).

[5] C. Andreani, D. Colognesi, J. Mayers, G. F. Reiter, and R. Senesi, Adv. Phys. **54**, 377 (2005).

[6] H. Rauh and N. Watanabe, Phys. Lett. **100A**, 244 (1984).

[7] M. P. Paoli and R. S. Holt, J. Phys. C **21**, 3633 (1988).

[8] J. Mayers, T. M. Burke, and R. J. Newport, J. Phys.: Condens. Matter **6**, 641 (1994).

[9] A. L. Fielding, D. N. Timms, and J. Mayers, Europhys. Lett. **44**, 255 (1998).

[10] M. Vos, Phys. Rev. A **65**, 012703 (2002).

[11] G. T. Orosz, G. Gergely, M. Menyhard, J. Tóth, D. Varga, B. Lesiak, and A. Jablonski, Surf. Sci. **566-568**, 544 (2004).

[12] D. Varga, K. Tokési, Z. Berényi, J. Tóth, and L. Kövér, Surf. Interface Anal. **38**, 544 (2006).

[13] D. Varga, K. Tökesi, Z. Berènyi, J. Tóth, L. Körvér, G. Gergely, and A. Sulyok, Surf. Interface Anal. **31**, 1019 (2001).

[14] L. van Hove, Phys. Rev. **95**, 249 (1954).

[15] J. Mayers and T. Abdul-Redah, J. Phys.: Condens. Matter **16**, 4811 (2004).

[16] M. Vos, C. Chatzidimitriou-Dreismann, T. Abdul-Redah, and J. Mayers, Nucl. Instrum. Methods Phys. Res. B **227**, 233 (2004).

[17] M. Vos, G. P. Cornish, and E. Weigold, Rev. Sci. Instrum. **71**, 3831 (2000).

[18] D. A. Shirley, Phys. Rev. B **5**, 4709 (1972).

[19] J. Mayers, T. M. Burke, and R. J. Newport, J. Phys.: Condens. Matter **6**, 641 (1994).

[20] A. L. Fielding, D. N. Timms, and J. Mayer, Europhys. Lett. **44**(2), 255 (1998).

[21] E. Weigold, A. S. Kheifets, V. A. Sashin, and M. Vos, Acta Crystallogr., Sect. A: Found. Crystallogr. **A60**, 104 (2004).

[22] M. Vos, G. Cooper, and C. Chatzidimitriou-Dreismann, in *Electron and Photon Impact Ionization and Related Topics*, edited by B. Piraux, Vol. 183 of Institute of Physics Conference Series (IOP, Bristol 2005), pp. 81–91.

[23] R. Bonham and G. de Souza, J. Chem. Phys. **79**, 134 (1983).

[24] T. Fujikawa, R. Suzuki, and Kövér, J. Electron Spectrosc. Relat. Phenom. **151**, 170 (2006).